ACS Biomaterials SCIENCE & ENGINEERING

Article

pubs.acs.org/journal/abseba

Cytocompatible Catalyst-Free Photodegradable Hydrogels for Light-Mediated RNA Release To Induce hMSC Osteogenesis

Cong Truc Huynh,[†,‡] Zijie Zheng,[†,‡] Minh Khanh Nguyen,[†,‡] Alexandra McMillan,[§] Gulen Yesilbag Tonga,[⊥] Vincent M. Rotello,[⊥] and Eben Alsberg*[,‡,∥]

[‡]Department of Biomedical Engineering, [§]Department of Pathology, and [∥]Department of Orthopaedic Surgery, Case Western Reserve University, 10900 Euclid Avenue, Cleveland, Ohio 44106, United States

[⊥]Department of Chemistry, University of Massachusetts, 710 North Pleasant Street, Amherst, Massachusetts 01003, United States

Supporting Information

ABSTRACT: Macroscopic hydrogels provide valuable platforms for controlling the release of genetic materials such as small interfering RNA (siRNA) and microRNA (miRNA) for biomedical applications. However, after these hydrogels are formed, it is challenging to alter the release rate of genetic materials. In this report, a Michael addition catalyst-free photodegradable poly(ethylene glycol) (PEG)-based hydrogel system has been developed that provides an active means of controlling the release of genetic materials postgelation using external UV light application. Photodegradation of photolabile linkages in the hydrogel network changes the hydrogel physiochemical properties such as swelling and degradation rate, augmenting the release rate of loaded genetic materials. In the absence of UV light, RNAs were released in a sustained fashion from both photodegradable and nonphotodegradable hydrogels. In contrast, RNA release rate from the photodegradable hydrogels was accelerated via UV light application, whereas it was not elevated with nonphotodegradable hydrogels. Regardless of the UV light exposure to the hydrogels, released siRNA against green fluorescent protein (siGFP) retained its bioactivity via effectively silencing GFP expression in destabilized GFP (deGFP)-expressing HeLa cells cultured in monolayer. Moreover, cells encapsulated in these hydrogels exhibited high cell viability, and loaded siGFP inhibited GFP expression of encapsulated deGFP-expressing HeLa cells with or without UV light application to the hydrogels. Importantly, released siRNA targeting noggin (siNoggin) and miRNA-20a from the hydrogels, with and without UV light application, induced osteogenic differentiation of human mesenchymal stem cells (hMSCs). This photodegradable hydrogel system may be a promising strategy for real-time, user-controlled release of genetic materials for tissue engineering and treatment of diseases such as cancer.

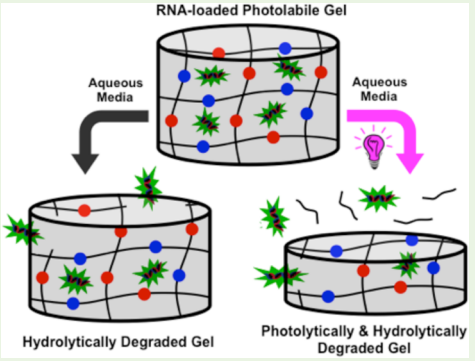

KEYWORDS: *miRNA, on-demand release, photolabile hydrogels, siRNA, stem cell differentiation, UV-controllable release, tissue regeneration*

1. INTRODUCTION

Mesenchymal stem cells (MSCs) possess a high capacity for self-renewal, immunomodulatory properties, and multipotentiality.[1−3] MSCs can be easily isolated from a variety of tissues such as placenta, bone marrow, muscle, fat, corneal stroma, and umbilical cord blood.[4−7] Among these, bone marrow-derived MSCs are a valuable, clinically relevant cell source for bone tissue engineering as they can be obtained in a minimally invasive manner via a bone marrow biopsy, and are capable of differentiating into connective tissue cells such as osteoblasts when exposed to specific microenvironmental conditions.[1,8−15] For example, the delivery of osteogenic molecules, such as bone morphogenetic protein-2 (BMP-2) and plasmid DNA encoding the growth factor, can drive MSC osteogenic differentiation.[8−11] However, supraphysiological amounts of BMP-2 are often needed to induce osteogenic differentiation in vivo,[16] and it is challenging to deliver plasmid DNA into the cell nucleus where it functions.[1,17,18]

RNA interference (RNAi) is a powerful biologic tool to post-transcriptionally silence gene expression in the cell cytoplasm using small interfering RNA (siRNA) and microRNA (miRNA). These RNA interfering molecules are promising for tissue regeneration and disease treatment due to their ability to block the synthesis of proteins that inhibit tissue development or induce disease progression.[1,18−23] siRNA and miRNA have been widely investigated for the treatment of cancer[23−26] and ischemia/reperfusion induced cardiac damage,[27] the regeneration of bone, cartilage, blood vessel, and fat[1,2,28−31]

Special Issue: Tissue Engineering

Received: December 20, 2016
Accepted: January 7, 2017
Published: January 7, 2017

DOI: 10.1021/acsbiomaterials.6b00796
ACS Biomater. Sci. Eng. 2017, 3, 2011−2023

Scheme 1. Schematic Showing the Formation of RNA/PEI Nanocomplexes and Hydrogel Fabrication via a Single Cross-Linked Michael Addition Reaction for Loading RNA

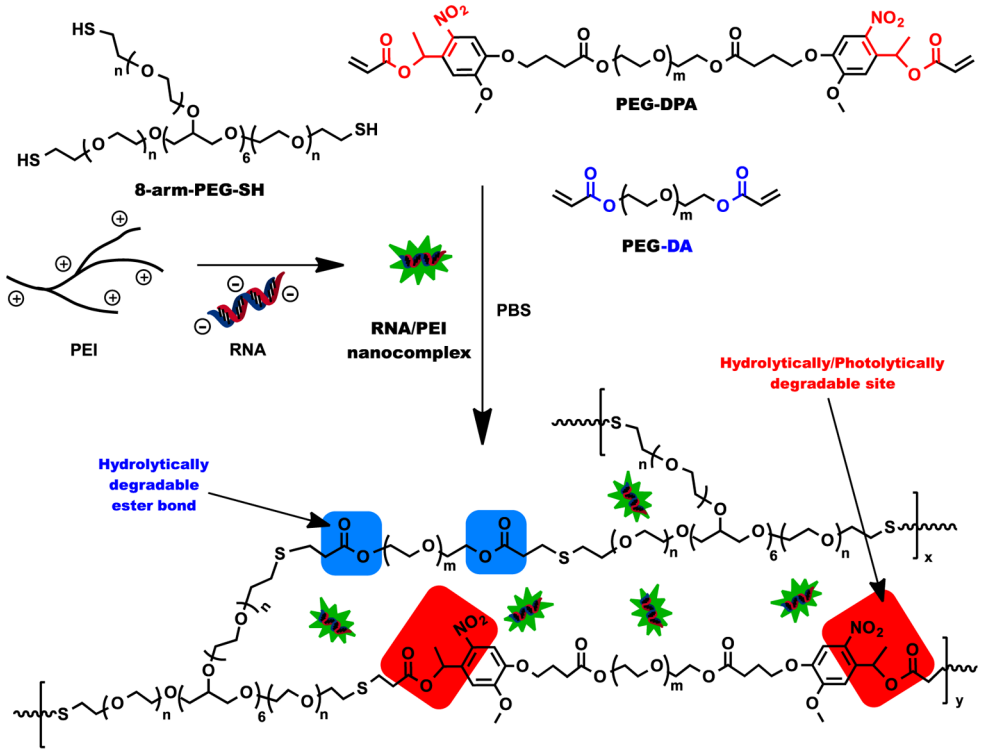

and wound healing.[32,33] Several RNAs have been identified as positive regulators of osteogenesis. For instance, miRNA-20a has been explored for enhancing osteogenic differentiation of human MSCs (hMSCs)[1,28] as it suppresses the expression of peroxisome-proliferator-activated receptor (PPARγ), Bambi and Crim1, which negatively affect BMP signaling in osteogenesis.[28,34] Alternatively, noggin is a protein that prevents osteogenic differentiation of hMSCs and impairs bone formation by blocking the binding of bone morphogenetic proteins (BMPs) to their receptors on the cell surface.[1,30,31] As a result, silencing the expression of the noggin gene using siRNA against the gene (siNoggin) can enhance osteogenic differentiation of MSCs and subsequently bone formation.[1,30,31]

siRNA and miRNA have been delivered to cells in naked form or through nanoparticles via their complexation with cationic polymers or incorporation into liposomes.[35−40] Unless these RNAs are chemically modified (modified RNA) to improve their stability and enable cell internalization, the use of naked unmodified RNAs is limited due to their intrinsic characteristics such as a short half-life in serum,[35−38] high susceptibility to degradation in the presence of ribonucleases,[37−40] rapid clearance by the renal system,[41] and poor cellular uptake owing to negative charge and high molecular weight.[35,39] Cationic polymers such as poly(ethylenimines) (PEIs),[39] chitosan,[41] poly(β-amino ester)[26] and others,[29,42] have been employed to complex negatively charged RNAs into nanoparticles via electrostatic interactions. These cationic nanoparticles bind to the negatively charged surface of cells followed by internalization, thus enhancing transfection efficiency. However, a major challenge for use of nanoparticles as a therapeutic modality is their rapid dispersion after administration in vivo, due to their small size, making it difficult to target sites of interest and to prolong gene silencing duration.[37,43−45]

Hydrogels are three-dimensional cross-linked polymer networks that have been extensively employed for local delivery of bioactive molecules, such as anticancer drugs, proteins, growth factors, and genes, in a sustained and/or controlled manner,[46−52] and they are useful for tissue regeneration strategies.[1,2,53−57] RNAs encapsulated into macroscopic hydrogels or scaffold biomaterials have been reported to provide sustained and localized delivery both in vitro and in vivo.[1,43−45,57−61] The release of RNAs from these biomaterials can be controlled through the regulation of many different factors, including the diffusion of RNA, biomaterial degradation rate, and affinity between RNA and hydrogels. However, these carriers do not permit precise control over RNA release and dosing at specific time points postimplantation into the body, which may reduce treatment efficacy if increased RNA presentation is deemed necessary after delivery vehicle implantation. Recent studies have demonstrated that an external, user-controlled stimulus in the form of UV light could be used to actively control and augment the release rate of siRNA from photodegradable polyethylene glycol (PEG) hydrogels at desired time points via simple UV application.[62,63] RNAs were loaded into the hydrogels via electrostatic interactions with covalently incorporated primary amine groups[62] or physical trapping in the form of RNA/PEI complexes.[63] Photolabile moieties were introduced to the PEG backbone for UV-controlled degradation of the hydrogel network, which permitted accelerated release rate of loaded RNA at designated time points. However, the potential of these hydrogel systems in tissue engineering applications may be restricted because of the use of catalysts necessary for hydrogel

DOI: 10.1021/acsbiomaterials.6b00796
ACS Biomater. Sci. Eng. 2017, 3, 2011−2023

formation, such as hydrogen peroxide, ammonium persulfate and tetramethylethylenediamine, which may negatively influence encapsulated cells.

This study presents a cytocompatible catalyst-free photodegradable hydrogel system that permits cell encapsulation and controlled release of loaded siRNA or miRNA, in the form of RNA/PEI complexes, postgelation via UV application. The photodegradable hydrogels were prepared via single-cross-linked Michael addition reaction between acrylate groups in poly(ethylene glycol)-diphotolabile-acrylate (PEG-DPA) and thiol groups in eight-arm PEG-thiol (PEG(-SH)$_8$) without the use of any catalyst.[64,65] Here, we examined whether application of UV light to hydrogel networks containing photodegradable linkages accelerated their degradation and subsequent release of RNA/PEI complexes compared to hydrogels lacking photodegradable moieties. The bioactivity of siRNA presented from these catalyst-free, photodegradable hydrogels in the absence or presence of UV light to monolayer cultured and encapsulated cells was investigated. Importantly, the potential application of this photodegradable hydrogel system for bone regeneration was also evaluated via the investigation of the capacity of released siNoggin and miRNA-20 to enhance osteogenic differentiation of hMSCs.

2. MATERIALS AND METHODS

2.1. Materials. PEG-DA and PEG-DPA were synthesized as previously reported[62,63,66] and detailed in Supporting Information. Branched PEI (*MW* 25 kDa), PEG (*MW* 4 kDa), 1-methoxyphenazine methosulfate (PMS), alizarin red S (ARS), high-glucose Dulbecco's modified Eagle medium (DMEM-HG), low-glucose DMEM (DMEM-LG), and anhydrous toluene were purchased from Sigma-Aldrich (St Louis, MO). G-418 (50 mg/mL) is a product of Hyclone Laboratories Inc. (Logan, UT), and was purchased from Fisher Scientific. 8-arm PEG thiol (PEG(-SH)$_8$) (MW 10 kDa, hexaglycerol core) was purchased from Jenkem Technology USA (Allen, TX).

siGFP (sequence 5′-GCA AGC UGA CCC UGA AGU UC-3′) and siRNA targeting luciferase (siLuc, sequence 5′-GAU UAU GUC CGG UUA UGU AUU-3′) are products of Dharmacon (Lafayette, CO), and were obtained from Thermo Fisher Scientific (Grand Island, NY). Prescreened fetal bovine serum (FBS, Gibco) and penicillin/streptomycin (P/S) were obtained from Fisher Scientific. siNoggin (sequence 5′-AAC ACU UAC ACU CGG AAA UGA UGG G-3′), miRNA-20a (sequence 5′-UAA AGU GCU UAU AGU GCA GGU AG-3′) and a nontargeting negative control siRNA (siCT, sequence 5′-UUC UCC GAA CGU GUC ACG UTT-3′) were purchased from Insight Genomics (Falls Church, VA). Quant-iT RiboGreen RNA reagent is product of Molecular Probes Inc. (Eugene, OR), and was obtained from Thermo Fisher Scientific. 3-(4,5-dimethyl thiazol-2-yl)-5-(3-carboxy methoxyphenyl)-2-(4-sulfo phenyl)-2H-tetrazolium (MTS) inner salt was obtained from Promega Corporation (Madison, WI).

2.2. Hydrogel Preparation and UV Dosage. The hydrogels were prepared through a single-cross-linked Michael addition reaction between thiol groups in PEG(-SH)$_8$ and acrylate groups in PEG-DA and/or PEG-DPA in PBS pH 7.4 at room temperature.[64,65] The PEG(-SH)$_8$ solution was added into the solution of PEG-DA and/or PEG-DPA at a 1:1 stoichiometric ratio of thiol to acrylate groups to obtain a desired polymer concentration. The mixture was vortexed for 10 s and then incubated at room temperature for 2 h to achieve gelation. A schematic depicting the formation of RNA/PEI nanocomplexes and an RNA-loaded hydrogel via thiol−acrylate Michael addition reaction is presented in Scheme 1.

Omnicure S1000 UV Spot Cure System (Lumen Dynamics Group, Mississauga, Ontario, Canada) was used as a UV source at intensities of ∼22.5 (low UV dose) and ∼45 (high UV dose) mW/cm^2. Note: UV intensities were measured as 2 and 10 mW/cm^2 for low and high UV doses, respectively, during the performance of this study using a UV meter that was later determined to be malfunctioning and supplying erroneous values. Once this was discovered, the UV intensities were remeasured to be ∼22.5 and ∼45 mW/cm^2 for low and high UV doses, respectively, based on the original instrument experimental setup parameters using a new and properly functioning UV meter. Although there may have been slight changes within the Omnicure UV instrument over time such as decreased bulb output, the UV intensities of ∼22.5 and ∼45 mW/cm^2 for low and high UV doses, respectively, more accurately represent those actually used in this study.

2.3. Gelation Time and Rheological Measurements. Gelation time was determined using the tube inverting method at room temperature, as previously described.[67] Briefly, the gelation time is the period from when the polymer solutions were mixed to the point when the mixture solution stopped flowing in the inverted tubes. The acrylate and thiol solutions (total 100 μL at desired concentration) were mixed in 1.7 mL microcentrifuge tubes, vortexed for 10 s and the gelation time was measured (N = 3).

The storage (G') and loss (G'') moduli of the mixed macromer solutions used to form hydrogels were measured using a dynamic Haake Mars III Rotational Rheometer (Thermo Fisher Scientific Inc., Waltham, MA). The thiol and acrylate polymer solutions were mixed together for 1 min, and then placed between two stainless steel parallel plates (8.0 mm diameter upper plate; 50 mm diameter lower plate) with a gap of 1.0 mm. The measurement was performed at 25 °C using oscillation time sweep mode with a controlled stress of 0.4 Pa and a frequency of 1.0 rad/s.[68]

2.4. Hydrogel Swelling and Degradation. To determine the swelling ratio and degradation profiles of hydrogels with and without UV exposure, we prepared 100 μL hydrogels in 1.7 mL microcentrifuge tubes as described in section 2.2, rinsed in diH2O overnight at 4 °C, froze them at −80 °C for at least 4 h, lyophilized, and then measured the initial dried weights (W_{do}).[1,43,68] The dried hydrogels were immersed in PBS (pH 7.4, 10 mL in 15 mL conical tubes) at 37 °C, which was changed every 3 days. Designated hydrogels were transferred onto the inside surface of the lid of a 10 cm Petri dish, and then exposed to a UV source with an intensity of ∼45 mW/cm^2 for 10 min (denoted as "UV 45−10") at 1 h after rehydration and then every week to determine the effect of UV exposure on the swelling ratio and degradation rate of the different hydrogels. At the predetermined time points, the designated hydrogels were collected and the uncollected "UV-treated" hydrogels were exposed to UV as mentioned earlier and then reimmersed in PBS. The wet weight (W_{wt}) of the collected hydrogels was measured, and the hydrogels were rinsed with diH_2O overnight at 4 °C, frozen at −80 °C and lyophilized to determine the dry weight (W_{dt}). The swelling ratio was calculated by W_{wt}/W_{do}, and the percentage mass loss was calculated by $(W_{do} - W_{dt})/W_{do} \times 100$.

2.5. Cytocompatibility of Degraded Hydrogels. To determine possible cytotoxicity of degraded hydrogel products, the viability of cells cultured with media containing various concentrations of these degradation products was determined using an MTS assay. Hydrogels (10%, w/w) prepared as described in section 2.2 were immersed in DMEM and then divided into two groups. The first group was incubated at 37 °C in the absence of UV light exposure to obtain hydrolytically degraded products. The media was not changed and the hydrogels were completely degraded at day 10. The second group was exposed to "UV 45−10", 6 times/day until the gels completely degraded (day 5) to obtain combined UV-degraded and hydrolytically degraded products. These degraded hydrogel products were incubated at 37 °C to reach the same incubation time as the samples in the first group (hydrolytic degradation group, day 10). The degradation products were then diluted with fresh DMEM to obtain designated concentrations. FBS was then added and their cytocompatibility was examined using deGFP-expressing HeLa cells and hMSCs.

deGFP-expressing HeLa cells (generously gift from Dr. Matthew Levy, Albert Einstein College of Medicine, Bronx, NY) were seeded in monolayer in 48-well plates (Fisher Scientific) at a density of 25,000 cells/well in 0.25 mL of DMEM-HG supplemented with 5% FBS and cultured at 37 °C and 5% CO_2 in a humidified incubator. After 1 day

DOI: 10.1021/acsbiomaterials.6b00796
ACS Biomater. Sci. Eng. 2017, 3, 2011−2023

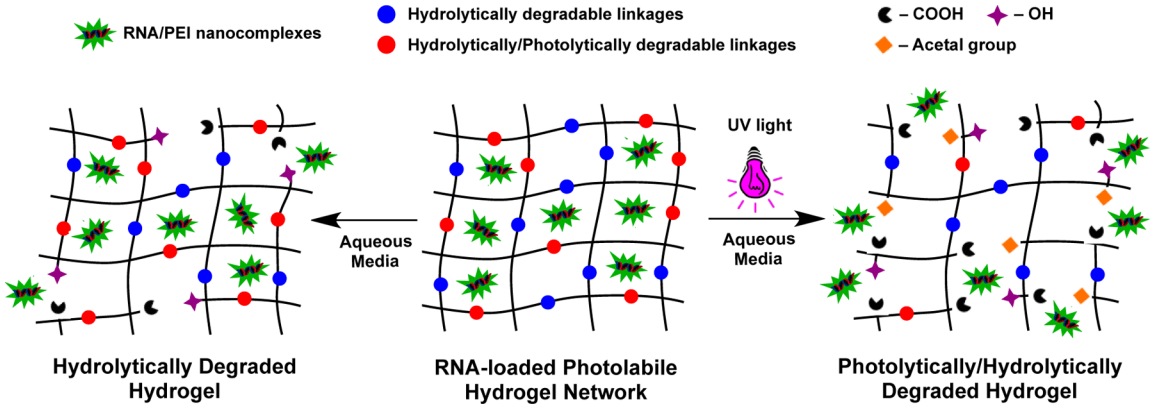

Figure 1. Schematic showing the release of RNA/PEI nanocomplexes from photolabile hydrogels in aqueous media in the absence or presence of an external UV light source.

of culture, the growth media was replaced with 0.25 mL DMEM-HG containing 2% FBS and various concentrations of degraded hydrogels. The cells were cultured for additional 2 days prior to the MTS assay.

hMSCs were isolated as previously reported[1] and stored under liquid nitrogen. The cells (passage 2) were thawed and plated into T175 flasks (Fisher Scientific) at a density of 5,000 cell/cm^2 and cultured at 37 °C and 5% CO_2 in a humidified incubator for 10 to 14 days before harvesting for further experiments. hMSCs were then seeded in monolayer in 48-well plates at a density of 15,000 cells/well (passage 3) in 0.25 mL of DMEM-LG supplemented with 10% FBS and 1% P/S. After 1 day of culture, the growth media was aspirated and replaced with 0.25 mL DMEM-LG supplemented with 5% FBS and 1% P/S and containing various concentrations of degraded hydrogels. The cells were cultured for an additional 4 days followed by the MTS assay.

To perform MTS assays, sterile solutions of MTS (2 mg/mL) and PMS (0.92 mg/mL) in PBS (pH 7.4) were prepared. Cell culture media in wells was aspirated and the cells were rinsed with 0.5 mL PBS. Fresh PBS (200 μL) was added into each well followed by the addition of 50 μL freshly prepared MTS/PMS mixture solution (1/20, v/v). Cells were then incubated for 2 h at 37 °C and 5% CO_2 in a humidified incubator. Then, 100 μL of the culture solutions was transferred into wells of 96-well plates, and absorbance at 490 nm was recorded using a VERSAmax microplate reader (Molecular Devices Inc., CA). Cells cultured with media only were designated as a control ("Ctrl") with 100% cell viability, and all other samples were normalized to "Ctrl".

2.6. Preparation of RNA/PEI Complexes. siRNA was diluted in nuclease free PBS (pH 7.4) to prepare a 100 μM stock solution. PEI was dissolved in nuclease free water at a stock concentration of 1 mg/mL (40 μM). siRNA/PEI complexes were prepared at an N/P ratio of 11.5, where N and P refer to the number of amine and phosphate groups in PEI and siRNA, respectively. A screening experiment showed that at the same final siGFP concentration, siGFP/PEI complexes prepared with low siGFP concentrations significantly enhanced GFP silencing levels (Figure S3, SI). However, a low concentration of siRNA/PEI complexes in a large volume of PBS is not ideal for loading a large amount of complexes into the hydrogels to measure release kinetics. Therefore, the siRNA/PEI complexes formed with a more concentrated solution of siRNA (6.4 μM) (method 1) was first chosen for examining siRNA release kinetics from the engineered photodegradable hydrogels. To prepare siRNA/PEI complexes using method 1, siRNA (12.8 μM) and PEI (9.6 μM) solutions were prepared separately in PBS. The siRNA solution was then added into the PEI solution (1/1, v/v), and the mixture was vortexed for 30 s and incubated at room temperature for 30 min to form the complexes. The siRNA/PEI complexes were then mixed with acrylated macromer solution, and the siRNA-loaded hydrogels (100 μL, 4 μg siRNA/gel) were fabricated as described in section 2.2 to examine the siRNA release kinetics.

Previous reports have demonstrated that lyophilized RNA/PEI complexes can retain their bioactivity by including lyo-protectants, such as sucrose[58] or trehalose,[29] in the complex solution prior to lyophilization. Lyophilized RNA/PEI complexes offer the ability to encapsulate large amounts of RNA within hydrogel or scaffold biomaterials. Lyophilized RNA/PEI complexes in the presence of sucrose prepared using a solution with a low RNA concentration (2.0 μM) (method 2) were shown to retain bioactivity of the RNA to a similar extent as nonlyophilized complexes (Figure S4). To prepare lyophilized RNA/PEI complexes (method 2), RNA (4.0 μM) and PEI (3.0 μM) solutions were prepared separately by diluting RNA and PEI stock solutions in PBS containing 10% sucrose. The RNA solution was added into the PEI solution (1/1, v/v), and the mixture was vortexed for 60 s and incubated at room temperature for 30 min to form the complexes. The complexes were then frozen at −80 °C for 2−4 h, lyophilized for at least 16 h, and then mixed with acrylated macromer solution. The RNA-loaded hydrogels were fabricated (50 μL, 5 μg RNA/gel) as described in section 2.2 to examine the RNA release kinetics in phenol red-free DMEM as well as the bioactivity of released RNA.

2.7. UV Light Triggered siRNA Release Kinetics in PBS. Freshly prepared siLuc/PEI complexes (method 1) were loaded into PEG-DA and/or PEG-DPA macromer solutions in 1.7 mL nuclease free tubes (Fisher Scientific) and the hydrogels (100 μL, 4 μg siRNA/gel) were prepared as described in section 2.2. Then, 1 mL of release solution (PBS, pH 7.4) was added into each tube and the release was carried out at 37 °C. At predetermined time points, the released media was collected and replaced with fresh media. Before adding release solution, "UV 45-10", was applied directly to the hydrogels in the UV exposure groups. In the presence of UV light application, the ester groups of the photolabile moieties photodegrade to create acetal and carboxylic acid groups,[69] which increases the degradation rate of the hydrogel and subsequently the release rate of loaded RNA. A schematic depicting the release of RNA/PEI nanocomplexes from photodegradable hydrogels in the absence or presence of external UV light exposure is presented in Figure 1. The released RNA was quantified using a RiboGreen RNA assay on a microplate reader (fmax, Molecular Devices Inc., CA) set for excitation at 485 nm and emission at 538 nm.[62] A series of known RNA concentrations in fresh release solution was used to establish a standard curve to calculate released RNA concentration. The release from blank hydrogels was carried out in parallel to eliminate effects of degraded polymers.

2.8. UV Light-Triggered RNA Release in Cell Culture Media and Bioactivity of Released RNA from Photodegradable Hydrogels. To investigate the bioactivity of released RNA, siGFP and siNoggin/miRNA-20a were employed for silencing GFP expression of deGFP-expressing HeLa cells and inducing osteogenic differentiation of hMSCs in monolayer, respectively. The lyophilized RNA/PEI complexes (method 2) were prepared and reconstituted in PEG-DA/PEG-DPA solution for fabrication of RNA-loaded "Photo-50" hydrogels (50 μL, 5 μg RNA/gel) as described in section 2.2. Prior

DOI: 10.1021/acsbiomaterials.6b00796
ACS Biomater. Sci. Eng. 2017, 3, 2011−2023

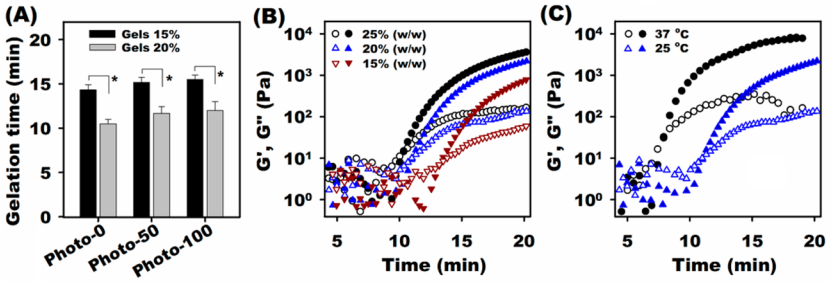

Figure 2. (A) Hydrogel gelation rates of different formulations as determined by the tube inverting method (* $p < 0.01$). (B, C) Time-dependent rheology of mixed "Photo-50", (B) different precursor solutions at 25 °C, and (C) 20% macromer solution at different temperatures. Storage (E', filled) and loss (E'', open) moduli are plotted as a function of time, and gelation time was determined as the time at which G' and G'' cross each other. At 25 °C, gelation time increased from 10.2 to 11.2, and then to 13.4 min when macromer concentration decreased from 25 to 20, and then to 15% (B). Gelation time of 20% macromer solution decreased from 11.2 to 8.2 min when the temperature increased from 25 to 37 °C (C).

to release studies, the hydrogels were rinsed with 0.5 mL phenol red-free DMEM at 4 °C for 3h to remove sucrose. The amount of RNA in the rinse solutions was measured and subtracted from the total amount initially loaded to obtain the actual RNA amount loaded for the release experiments. Less than 5% of the total amount originally loaded was measured in the rinse solutions. The release of RNAs into phenol red-free DMEM (0.5 mL, DMEM-HG for siGFP and DMEM-LG for siNoggin and miRNA-20a) was carried out in the absence and presence of UV light exposure. The release samples were collected every 2 days and fresh media were added. Designated hydrogels were directly exposed to UV at an intensity of ~22.5 mW/cm^2 for 10 min ("UV 22−10") every day. The RNA concentration in releasates was quantified as described in section 2.7.

2.8.1. Capacity of Released siGFP to Silence GFP Expression in deGFP-Expressing HeLa Cells Cultured in Monolayer. deGFP-expressing HeLa cells were seeded in monolayer in 24-well plates (Fisher Scientific) at a density of 50,000 cells/well in 0.5 mL of DMEM-HG supplemented with 5% FBS and G-418 (250 μg/mL) and cultured at 37 °C and 5% CO_2 in a humidified incubator. After 1 day of culture, the growth media was aspirated and replaced with 0.5 mL of transfection solutions, which were prepared by diluting the pooled releasates from 3 hydrogels at specific time points with fresh DMEM-HG (1:2, v/v). The cells were cultured with the transfection solutions for 6 h, after which the transfection media was replaced with 0.5 mL of fresh culture media without G-418. The cells were then cultured for 2 more days, and harvested for flow cytometry (EPICS XL-MCL, Beckman Coulter, Fullerton, CA) to quantify the degree of GFP silencing. Freshly reconstituted lyophilized siGFP/PEI complexes in DMEM-HG were used as a positive control ("Pos. Ctrl"). Cells cultured with media only served as a control with 100% GFP expression ("Ctrl"), and all other groups were normalized to the "Ctrl".

2.8.2. Driving Osteogenic Differentiation of hMSCs in Monolayer. hMSCs (passage 3) were seeded in monolayer in 24-well plates at a density of 10,000 cells/well in 0.5 mL of DMEM-LG supplemented with 10% FBS and 1% P/S. After 1 day of culture, growth media was replaced with 0.5 mL DMEM-LG containing the same concentration of freshly reconstituted or released RNA/PEI complexes (40 nM, siNoggin or miRNA-20a) and culture continued for 6 h. The transfection media was then replaced with 0.5 mL osteogenic media, which is DMEM-LG supplemented with 10% FBS, 1% P/S, 100 nM dexamethasone (MP Biomedicals, Solon, OH), 10 mM b-glycerophosphate (CalBiochem, Billerica, MA), and 100 μM ascorbic acid (Wako USA, Richmond, VA). The osteogenic media was changed twice per week. After 3 weeks of culture, osteogenic media was removed and cells were rinsed with 0.5 mL PBS, fixed with ice-cold ethanol 70% in diH_2O (v/v) at 4 °C for 1 h followed by rinsing with 0.5 mL diH_2O. The cells were then stained with ARS solution (60 mM, pH 4.1) for 10 min, rinsed twice with 0.5 mL of diH_2O, and then rinsed for 15 min with 0.5 mL of PBS pH 7.4 prior to light microscopy imaging using a TMS-F microscope (Nikon, Japan) equipped with a Nikon E995 camera (Nikon, Japan). Calcium-bound dye in each well was dissolved with 0.5 mL 10% (w/v) cetylpyridinium chloride (CPC, Sigma) in 10 mM sodium phosphate buffer at pH 7.0 for 20−30 min at room temperature. Then, 100 μL of the solution was placed into wells of 96-well plates, and the ARS concentration was quantified by measuring absorbance at 562 nm on a VERSAmax microplate reader (Molecular Devices Inc., CA). Cells transfected with DMEM-LG only, freshly reconstituted lyophilized RNA/PEI and siCT/PEI complexes in DMEM-LG were used as a control ("Ctrl"), a knockdown positive Ctrl ("Pos. Ctrl") and a negative Ctrl ("Neg. Ctrl") group, respectively. The ARS concentrations in PBS solution containing 10% (w/v) CPC (pH 7.0) were reported to be linearly related to the absorbance of the ARS solutions[70,71] and bound calcium amounts;[72] and therefore the absorbance ratios between groups are considered to be their deposited calcium ratios.

2.9. Silencing Gene Expression of Encapsulated deGFP-Expressing HeLa Cells in siGFP-Loaded Photodegradable Hydrogels. To examine the ability of loaded-siRNA in the hydrogels to silence encapsulated cells' gene expression, we encapsulated deGFP-expressing HeLa cells (1×10^7 cells/mL gel) and methacrylated cell adhesion oligopeptide Gly-Arg-Gly-Asp-Ser-Pro prepared as previously reported[73] (0.5% (w/w) dry polymer, Commonwealth Biotechnologies, Richmond, VA) into 15% (w/w) photodegradable hydrogels with or without lyophilized siRNA/PEI complexes (20 μg siRNA/mL gel). The hydrogels were formed between 2 glass plates with 400 μm spacers for 20 min and then punched out using a 6 mm biopsy punch, and each individual 6 mm hydrogel was immersed in 0.5 mL of DMEM-HG in wells of 24-well plates and incubated at cell culture conditions for 1 h to remove sucrose. The media was then replaced by DMEM-HG supplemented with 5% FBS and cultured for 2 days. Two and twenty-four hours after preparation, designated hydrogels were scooped out of the wells, placed in Petri dishes and exposed to "UV 22−10". After 2 days of culture, GFP expression of the encapsulated cells was assessed using confocal microscopy (LSM510, Zeiss, Jena, Germany). Images were taken every 5 μm in the z direction for 50 μm from the bottom of the hydrogels and compiled into a single 3D projection.

2.10. Statistical Analysis. The data are expressed as mean ± standard deviation ($N = 3$). Statistical analysis was performed with one-way analysis of variance (ANOVA) with Tukey−Kramer Multiple Comparisons using GraphPad Instat 3.0 software (GraphPad Software Inc., La Jolla, CA). $P < 0.05$ was considered statistically significant.

3. RESULTS AND DISCUSSION

3.1. Hydrogel Preparation. Hydrogels were prepared by mixing PBS solutions of PEG(-SH)$_8$ with PEG-DA and/or PEG-DPA at room temperature. Three different hydrogel compositions were prepared in this study: "Photo-0", "Photo-50" and "Photo-100" hydrogels. The nomenclature was assigned based on the PEG-DPA weight percentage of the total acrylated macromers in each condition. The non-photodegradable "Photo-0" hydrogels, formed by mixing

DOI: 10.1021/acsbiomaterials.6b00796
ACS Biomater. Sci. Eng. 2017, 3, 2011−2023

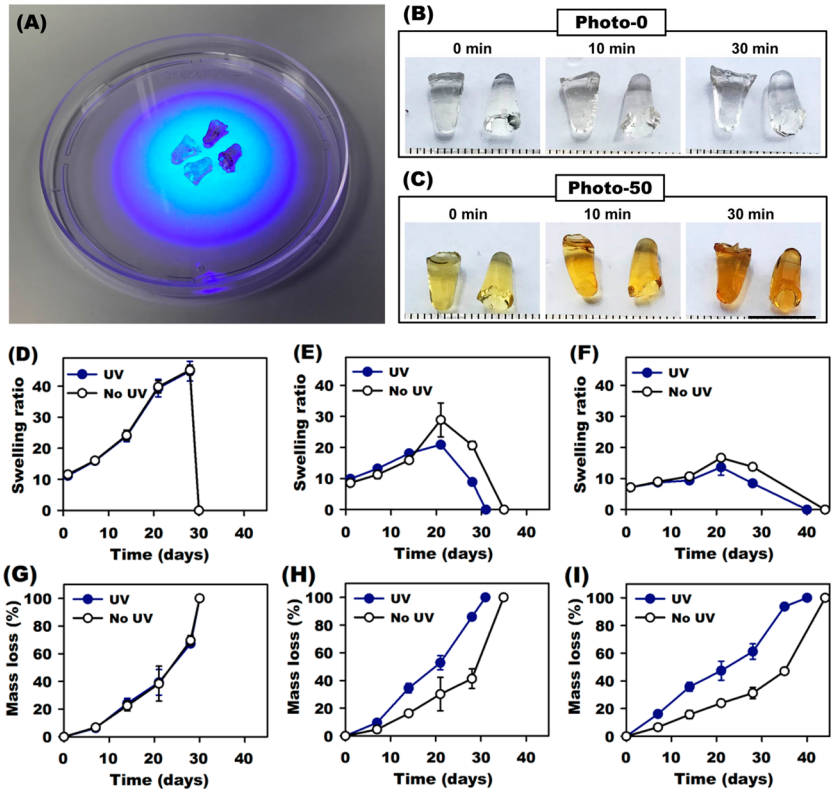

Figure 3. (A) Photograph of the hydrogels placed onto the inside surface of a 10 cm Petri dish lid under UV light exposure. (B, C) Photographs of (B) "Photo-0" and (C) "Photo-50" hydrogels (100 μL macromer solutions were gelled in 1.7 mL microcentrifuge tubes) before and after being exposed to UV light at an intensity of ~45 mW/cm^2 for 10 and 30 min. The scale bar indicates 1 cm. (D−F) Swelling ratio and (G−I) degradation kinetics of 20% (w/w) (D, G) "Photo-0", (E, H) "Photo-50" and (F, I) "Photo-100" hydrogels in the absence or presence of "UV 45−10") weekly.

PEG-DA and PEG(-SH)$_8$ solutions, did not contain photodegradable PEG-DPA macromer and were not responsive to UV light. The photodegradable "Photo-50" hydrogels were formed by mixing a mixture of PEG-DA and PEG-DPA (1/1, w/w) with PEG(-SH)$_8$, and the photodegradable "Photo-100" hydrogels were formed by mixing solutions of PEG-DPA with PEG(-SH)$_8$. Gelation times of prepared hydrogels were determined using the previously reported tube inverting method[67] (Figure 2A) and rheological assessment[68] (Figure 2B). Increasing density of photolabile moiety resulted in slightly longer, but not significant, gelation time (Figure 2A), likely due to the steric hindrance of aromatic rings in the photolabile groups. Increasing macromer concentration significantly decreased gelation time (Figure 2). In addition, the gelation time decreased with increasing the cross-linking temperature (Figure 2C).

3.2. Hydrogel Swelling and Degradation. In situ forming hydrogels provide valuable platforms for encapsulation of bioactive factors and/or cells for drug delivery and tissue regeneration applications.[48,74] Hydrogel swelling and degradation result in increased network pore size, which plays a key role in controlling release of encapsulated bioactive factors, providing space for newly forming tissues and increasing the rate of nutrient and oxygen transport to incorporated cells and waste removal.[54−56] In this photodegradable hydrogel system, swelling and degradation properties can be tailored through UV light exposure and/or changing the density of photolabile moieties in the hydrogels. Hydrogels were placed onto the inside surface of a 10 cm Petri dish lid (Figure 3A), and upon the application of UV light, the color of "Photo-0" hydrogels did not change (Figure 3B), whereas "Photo-50" hydrogels changed from light yellow to dark yellow, and then to slightly brown (Figure 3C). The swelling ratio and degradation profiles of 20% (w/w) hydrogels in the absence and presence of "UV 45−10" were determined (Figure 3). As expected, swelling ratio and degradation profiles of "Photo-0" hydrogels were not influenced by UV light exposure (Figure 3D, G). The swelling ratio and mass loss of "Photo-0" hydrogels gradually increased almost linearly over 4 weeks, and the swelling reached maximum at day 28 before the hydrogels were completely degraded at day 30. Interestingly, the swelling ratio and degradation profiles of "Photo-50" and "Photo-100" hydrogels were strongly affected by UV irradiation (Figure 3E, F, H, I). After 24 h equilibration swelling, the swelling ratios of "Photo-50" hydrogels increased in an almost linear fashion in the first 2 weeks regardless of the presence or absence of UV light. The swelling ratio of "No UV" hydrogels then rapidly increased to reach a maximum value at day 21, whereas the swelling ratio of "Photo-50" "UV" hydrogels slightly increased (Figure 3E). A similar trend of swelling ratio was also observed in "Photo-100" hydrogels (Figure 3F), with lower maximum swelling ratios compared to the "Photo-50" hydrogels. This behavior is likely due to the increased hydrophobicity of the "Photo-50" and "Photo-100" hydrogel networks caused by the increased density of aromatic group-containing photodegradable groups. The degradation rate of the "Photo-50" and "Photo-100" hydrogels was also accelerated through the application of UV light compared to that of their "No UV" counterparts, indicating the photodegradation of photolabile groups in the hydrogel network (Figure 3H, I). Without UV irradiation, "Photo-50"

DOI: 10.1021/acsbiomaterials.6b00796
ACS Biomater. Sci. Eng. 2017, 3, 2011−2023

and "Photo-100" hydrogels showed similar trends in degradation with slow degradation rates in the first 4 weeks, followed by a rapid increase in hydrolytic degradation that led to their complete degradation by days 35 and 44, respectively. In contrast, with UV application, "Photo-50" and "Photo-100" hydrogels showed more rapid degradation rates with their complete degradation by days 31 and 40, respectively. In addition, by increasing the density of photodegradable moieties ("Photo-0" to "Photo-50" to "Photo-100"), the hydrolytic degradation rate of hydrogels decreased due to an increase in the hydrogel hydrophobicity. The swelling ratio of the "No UV"-treated "Photo-50" and "Photo-100" hydrogels was higher than that of the corresponding "UV"-treated hydrogels after 2 weeks (Figure 3E, F). This observation may be attributed to the photodegradation and increased concentration of degraded products in the surrounding PBS as these hydrogels degraded more rapidly (Figure 3H, I).

3.3. Cytocompatibility of Hydrogel Degradation Products. In aqueous media, without UV irradiation the ester groups of the photodegradable hydrogels are hydrolyzed to form carboxylic acid and hydroxyl groups. However, upon UV application the ester groups of the photodegradable moieties in PEG-DPA underwent photodegradation to form the acetal derivative and free carboxylic acid groups.[69] To determine cytocompatibility of the hydrogel degradation products containing the above-mentioned chemical groups, we examined the viability of cells exposed to culture media containing different concentrations of the degradation products using an MTS assay. The degraded products exhibited minimal toxicity to both HeLa cells and hMSCs at low concentrations (Figure 4). The average viability of both cell types decreased below 70% when cells were cultured with media containing more than 2 mg/mL of degradation products. At most hydrogel degradation product concentrations, the viability of cells exposed to photodegraded hydrogels was slightly lower, but not significantly, than that of those exposed to hydrolytically degraded products, which may be a result of the acetal groups produced via photodegradation. In a photolabile hydrogel system with the same photodegradable moiety, UV application (10 mW/cm^2 for total 16 min) and hydrogel photodegraded products were also reported to show a minimal effect on the viability of encapsulated hMSCs.[69]

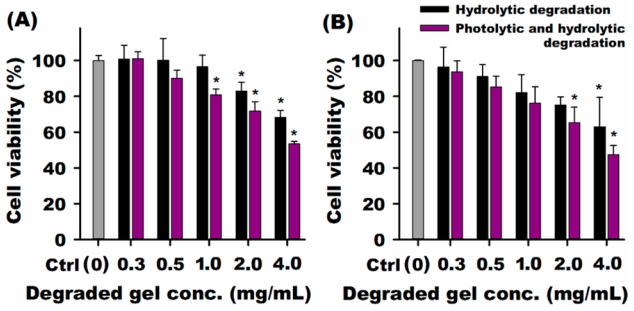

Figure 4. Viability of (A) HeLa cells and (B) hMSCs cultured with the degradation products of "Photo-50" hydrogels as measured using MTS assay. * $p < 0.05$ compared to corresponding "Ctrl" groups.

3.4. UV Light Triggered siRNA Release into PBS. To investigate the effect of UV light exposure on the release kinetics of siRNA from photodegradable hydrogels, we examined the release of siRNA/PEI complexes from "Photo-0" (Nonphotolabile), "Photo-50", and "Photo-100" into nuclease-free PBS in the absence and presence of UV light exposure. As expected, siRNA was gradually released at a similar rate from "Photo-0" hydrogels regardless of UV exposure over the course of 31 days (Figure 5A), indicating UV-independent release kinetics. The siRNA release was likely governed by the hydrolytic degradation of ester groups in the hydrogel networks.[62] Importantly, the release of siRNA from both "Photo-50" and "Photo-100" hydrogels was strongly influenced by the application of external UV light (Figure 5B, C). In particular, without UV exposure, siRNA was retained in the hydrogel network and released slowly in the first 3 weeks with less than 25% of siRNA cumulatively released. The release rate then rapidly increased after 3 weeks due to an increase in ester group hydrolysis rate in the networks. Upon the complete degradation of the hydrogels, all loaded siRNA was released by days 38 and 46 for "Photo-50" and "Photo-100" hydrogels, respectively. In contrast, siRNA release rate from the UV-treated ("UV") hydrogels was substantially accelerated after the second dose of UV (day 7) because of the contribution of photodegradation of photolabile moieties in the hydrogel networks (Figures 5B, C). Although "Photo-50" UV-treated hydrogels were fully degraded and released all loaded siRNA by day 33, "Photo-100" UV-treated hydrogels released most of the loaded siRNA by day 35 with complete degradation by day 46. The hydrogels with a lower photolabile moiety density presented shorter hydrogel persistence time likely due to faster hydrolytic degradation rate of the ester groups in the less hydrophobic hydrogel networks. These results are supported by degradation properties of the corresponding hydrogels (Figure 3). Taken together, this photodegradable hydrogel system is able to retain siRNA for a prolonged period of time, and the release of the loaded siRNA can actively accelerate the introduction of photodegradable linkages into the hydrogels and subsequent application of UV light.

For almost a decade, control over the localized and/or sustained release of RNA using macroscopic hydrogel and scaffold biomaterials has been investigated.[1,26,29,32,43−45,58−61]

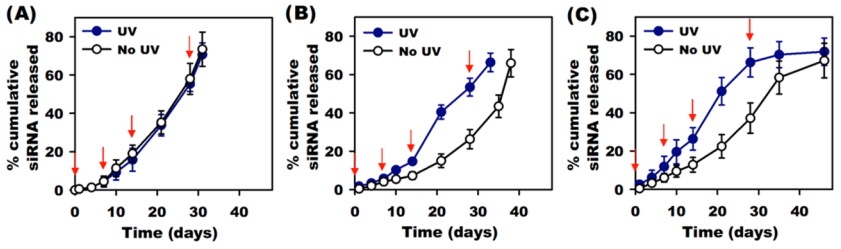

Figure 5. siRNA release profiles from 20% (w/w) (A) "Photo-0", (B) "Photo-50", and (C) "Photo-100" hydrogels in the absence and presence of "UV 45−10". The (red) arrows denote the time points when UV was applied to the hydrogels.

DOI: 10.1021/acsbiomaterials.6b00796
ACS Biomater. Sci. Eng. 2017, 3, 2011−2023

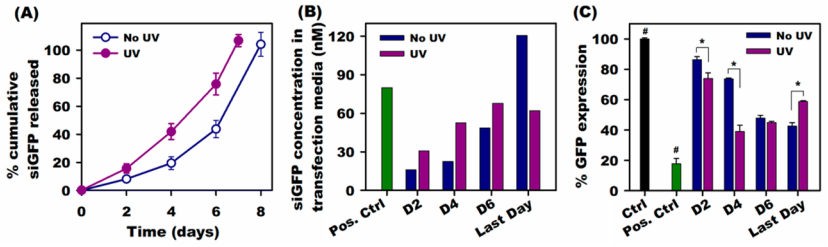

Figure 6. (A) Release profiles of lyophilized siGFP/PEI complexes (method 2) from 20% (w/w) "Photo-50" hydrogels in the presence or absence of "UV 22−10" everyday. (B) Concentration of siGFP in the transfection media used in the bioactivity study, and (C) GFP expression of monolayer-cultured deGFP-expressing HeLa cells transfected with releasates collected at predetermined time points. # $p < 0.01$ compared to all other groups, * $p < 0.01$.

The release of RNAs from these biomaterial systems can be predicted and adjusted by controlling the degradation rate of the biomaterials and/or the diffusivity of the RNA through the network[1,26,29,32,43−45,58,59] by changing, for example, macromer concentration and/or the degree of functionalized RNA-affinity molecules[43−45,60] before gelation. However, the release from these systems cannot be altered by physician or patient after the biomaterials are injected or implanted into the body. Recent studies have reported that the use of external, user-controlled stimulus in the form of UV light at desired time points could actively control hydrogel degradation rate and therefore the release of loaded RNA.[62,63] The electrostatic interaction between negatively charged RNA and hydrogel-conjugated positively charged primary amine groups[62] or physically trapped RNA in the form of RNA/PEI nanocomplexes[63] helped retain RNA in the hydrogel network. Upon the application of UV light, the photolabile linkages underwent photodegradation, which resulted in the breakdown of the hydrogel network and release of loaded RNA. However, the requirement of catalysts in these previously reported hydrogel preparations may affect the survival of the encapsulated cells. In contrast, the cytocompatible, photodegradable catalyst-free hydrogel system reported here provides a flexible, active method to control the "on demand" delivery of RNA/PEI nanocomplexes at designated time points with a user-controlled UV light source and permits encapsulation of cells with high cell viability for regulation of gene expression and tissue regeneration applications.

3.5. Capacity of Released siGFP to Silencing GFP Expression in deGFP-Expressing HeLa Cells in Monolayer. After demonstrating that the hydrogel system could accelerate siRNA release upon UV application, the bioactivity of the released siRNA was then examined. To do this, lyophilized siGFP/PEI complexes (method 2) were prepared and loaded into 20% (w/w) "Photo-50" hydrogels (50 μL, 5 μg siGFP/gel). The released siGFP into media with and without UV application was then quantified and applied to deGFP-expressing HeLa cells cultured in monolayer.

First, the release profiles of siGFP from 20% (w/w) "Photo-50" hydrogels into phenol red-free DMEM-HG were measured (Figure 6A). In the absence of UV light, siRNA gradually released from "No UV" hydrogels with a cumulative release of 20% over the first 4 days. The release rate increased after day 4 and all loaded-siRNA was released by day 8 when the hydrogels were completely hydrolytically degraded. As expected, when exposed to UV, "UV" hydrogels released siRNA at a faster rate (Figure 6A), and all loaded siRNA was released by day 7 upon complete degradation of the hydrogels. Interestingly, regardless of the absence or presence of UV light exposure, the persistence time of "Photo-50" hydrogels in DMEM-HG is much shorter than in that of the hydrogels in PBS (more than 33 days, Figure 6B). It is not clear how the differences in composition between PBS and DMEM-HG, the latter of which contains glucose, would lead to differences in the hydrolysis rate of the ester groups in the hydrogel network and subsequent persistence times of the hydrogels. This finding is consistent with other work in the literature,[61,63,75] which reported that DMEM accelerated hydrolytic degradation of ester groups within hydrogels compared to PBS.

The releasates from three different hydrogels at each specific time point were combined, diluted 1:2 (v/v) with fresh DMEM-HG and used to treat deGFP-expressing HeLa cells in monolayer to examine their ability to silence GFP expression. The siRNA concentrations used for transfection are presented in Figure 6B. As shown in Figure 6C, whereas cells cultured with media served as a control group ("Ctrl") with 100% GFP expression, and all other conditions were normalized to this group. Cells treated with releasates from both "UV" and "No UV" hydrogels showed a significant reduction in GFP expression compared to "Ctrl", indicating the bioactivity of released siGFP (Figure 6C). Specifically, cells cultured with freshly reconstituted lyophilized siGFP/PEI complexes, a knockdown positive control ("Pos. Ctrl"), had reduced GFP expression compared to all other groups (Figure 6C) due to the high siRNA concentration (80 nM) in the transfection media (Figure 6B). At day 2 and 4 (D2 and D4), cells transfected with releasates from "UV" hydrogels showed lower GFP expression than that of cells treated with releasates from "No UV" hydrogels (Figure 6C) because more siRNA (1.92 and 2.32 fold in siRNA concentration for D2 and D4, respectively; Figure 6B) was released from the "UV" hydrogels at those time points. At day 6 (D6), no difference in the degree of GFP expression of the transfected cells was observed between "UV" and "No UV" hydrogels due to the smaller relative difference (1.39 fold higher siRNA concentration in "UV" group at D6; Figure 6B) in siGFP concentration in the transfection media. At the last time point ("Last Day", day 7 for "UV" gels and day 8 for "No UV" gels), cells transfected with these releasates from "No UV" hydrogels showed lower GFP expression than those treated with releasates from "UV" hydrogels (Figure 6C) as a result of the higher siGFP concentration in the "No UV" releasates.

Although the released siGFP could inhibit GFP expression, there was a reduction in the bioactivity of released siGFP at the later time points (D6 and the last day). For example, siGFP concentration in releasates from "No UV" hydrogels at the last day was higher than that from the same hydrogels at D6 or in the "Pos. Ctrl" (Figure 6B). However, the degree of GFP silencing was similar and lower than that of D6 and "Pos. Ctrl",

DOI: 10.1021/acsbiomaterials.6b00796
ACS Biomater. Sci. Eng. 2017, 3, 2011−2023

respectively (Figure 6C). A similar phenomenon was also observed in the "UV" hydrogels. Although the siGFP concentration is similar in releasates of D4, D6, and last day, cells transfected with the releasates from the last day expressed GFP at a higher level compared to other conditions. This reduction in bioactivity of released siGFP at the later time points could be attributed to the binding of carboxylic acids in the hydrogel degradation products to the siRNA/PEI nanoparticles, resulting in increased particle size and decreased positive surface charge density. As a result, the capacity of the siRNA/PEI nanocomplexes to interact with the cells would decrease, leading to a reduction in the degree of gene silencing. Supporting this theory, it was previously reported that the binding of anionic polymers into positively charged nanoparticles increases particle size and decreases surface charge density,[76,77] leading to lower cellular internalization capacity.[78] To confirm this hypothesis in the current system, we freshly reconstituted lyophilized siGFP/PEI powder with D6 releasates from empty "UV" hydrogels (without siGFP) and then cultured with deGFP-expressing HeLa cells. It was found that the GFP silencing capacity of lyophilized siRNA/PEI complexes decreased from 82% to 56% and 52% after mixing with hydrogel degradation products and incubating at 37 °C for 30 min and 3 days, respectively (Figure S5). Moreover, cells treated with releasates from the empty "UV" hydrogels (without siRNA) expressed similar GFP levels compared to "Ctrl" (Figure S5), indicating that the hydrogel degradation products did not affect GFP expression. Taken together, although a slight reduction in bioactivity of released siGFP was observed at the later time points, the released siGFP from this new photodegradable hydrogel system retained its bioactivity by silencing GFP expression of deGFP-expressing HeLa cells cultured in monolayer regardless of the absence or presence of UV light exposure.

3.6. Silencing Gene Expression of deGFP-Expressing HeLa Cells Encapsulated in siGFP-Loaded Photodegradable Hydrogels. As described earlier, this cytocompatible, photodegradable catalyst-free hydrogel system permits encapsulation of cells with high cell viability for regulation of gene expression. To confirm the ability to silence gene expression of encapsulated cells in the photodegradable hydrogel system, deGFP-expressing HeLa cells were encapsulated to the 15% (w/w) "Photo-50" hydrogels with and without lyophilized siRNA/PEI complexes and cultured for 2 days, followed by the examination of GFP expression using confocal microscopy. The cells encapsulated in the hydrogels without siGFP or with nontargeting siLuc expressed strong GFP signal regardless of the presence or absence of UV light (Figure 7). In contrast, the cells encapsulated in the hydrogels containing siGFP expressed less intense GFP signal in both "No UV" and "UV" hydrogels (Figure 7), demonstrating the inhibitory effect of the encapsulated siGFP. The ability of loaded siGFP in the hydrogels to silence GFP expression of encapsulated deGFP-expressing cells has been reported previously[1,43,44,58] to demonstrate the bioactivity of the genetic material. There was no difference in the degree of GFP expression between "No UV" and "UV" hydrogels (Figure 7), which indicates that the UV light is benign with respect to the bioactivity of loaded siGFP. Moreover, the encapsulated cells in both "UV" and "No UV" hydrogels showed high cell viability via live−dead staining after 2 days culture (Figure S6), indicating that the experimental process, UV light dose, hydrogel materials, and hydrogel degradation products are not toxic to encapsulated cells.

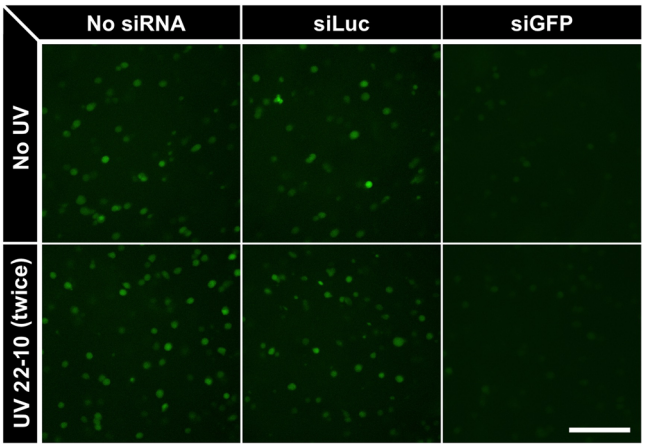

Figure 7. Representative confocal fluorescence microphotographs depicting the GFP signal of encapsulated deGFP-expressing HeLa cells (1×10^7 cells/mL gel) in 15% (w/w) "Photo-50" hydrogels loaded with siRNA (20 μg/mL) in the absence or presence of UV light exposure. The scale bar indicates 200 μm.

3.7. Inducing hMSC Osteogenic Differentiation with Released siNoggin/miRNA-20a. After demonstrating the capacity of the photodegradable hydrogels to accelerate RNA release in response to UV light while retaining RNA bioactivity, we examined the ability of released RNA to regulate stem cell differentiation to demonstrate the potential of the hydrogel system in tissue regeneration. Therefore, the ability of osteogenic RNA, specifically siNoggin and miRNA-20a, released from the photodegradable hydrogels to induce the osteogenic differentiation of hMSCs cultured in monolayer was examined. Lyophilized siNoggin/PEI or miRNA-20a/PEI nanocomplexes were encapsulated in the photodegradable hydrogels to determine their release kinetics and bioactivity. First, the release kinetics of siNoggin from 15% (w/w) "Photo-50" hydrogels into phenol red-free DMEM-LG in the absence or presence of UV light was examined (Figure 8A). siNoggin was released gradually from "No UV" hydrogels in a sustained manner with 55% cumulatively released over the first 10 days and complete release by day 12 coinciding with total degradation of the hydrogels. In contrast, siNoggin was released from "UV" hydrogels at a much faster release rate than from "No UV" hydrogels (Figure 8A), and all loaded siNoggin was released by day 10 upon complete hydrogel degradation.

To determine the ability of the released siNoggin to induce hMSC osteogenic differentiation, it was applied to hMSCs cultured in monolayer. The cells were then cultured in osteogenic media for 3 weeks and deposited calcium was quantified. The "Ctrl" group transfected with DMEM-LG only exhibited low calcium staining (Figure 8B). The hMSCs treated with nontargeted control siCT ("Neg. Ctrl") and releasates from empty "UV"-treated hydrogels ("Gel Only") exhibited a similar degree of calcium deposition to that of "Ctrl" (Figure 8B). These results were confirmed by calcium quantification (Figure 8C). In contrast, cells transfected with lyophilized siNoggin ("Pos. Ctrl"), a knockdown positive control and with released siNoggin from the photolabile hydrogels at different time points showed increased calcium deposition (Figure 8B), illustrating that the released siNoggin induced osteogenic

DOI: 10.1021/acsbiomaterials.6b00796
ACS Biomater. Sci. Eng. 2017, 3, 2011−2023

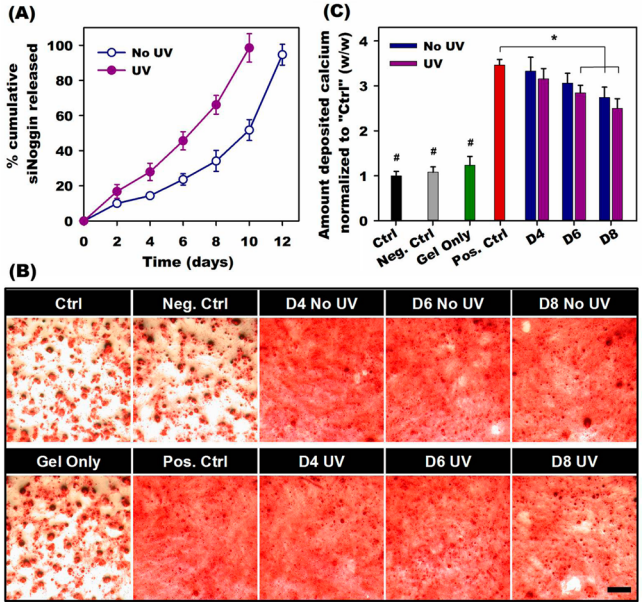

Figure 8. (A) Release profiles of siNoggin from 15% (w/w) "Photo-50" hydrogels into phenol red-free DMEM-LG in the absence or presence of "UV 22−10" applied daily. (B) Representative photomicrographs of ARS stained cells showing the deposition of calcium, and (C) quantification of deposited calcium (normalized to "Ctrl") by hMSCs cultured in monolayer and transfected with released siNoggin from hydrogels at days 4, 6, and 8 (D4, D6 and D8, respectively), or freshly reconstituted lyophilized siRNA/PEI complexes of siCT ("Neg. Ctrl") or siNoggin ("Pos. Ctrl") (RNA 40 nM). "Gel Only": pooled D6 releasates from "UV"-treated hydrogels lacking siRNA. # $p < 0.01$ compared to groups that do not contain the same symbol, * $p < 0.05$. The scale bar indicates 200 μm.

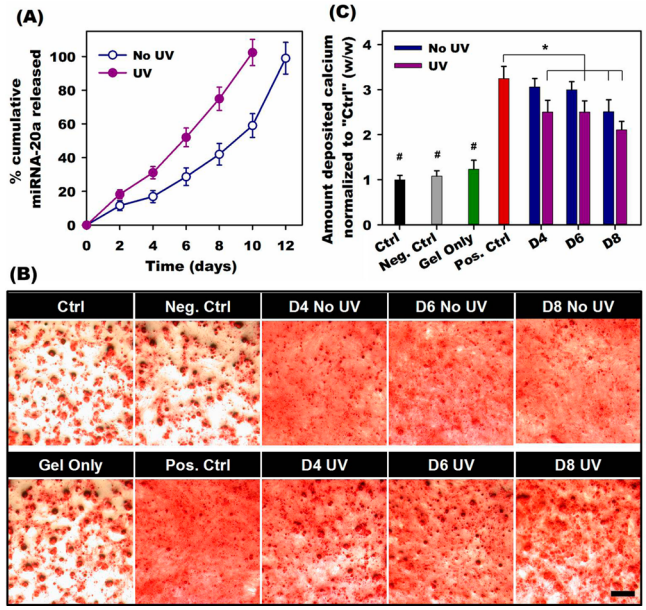

Figure 9. (A) Release profiles of miRNA-20a from 15% (w/w) "Photo-50" hydrogels into phenol red-free DMEM-LG in the absence or presence of "UV 22−10" applied daily. (B) Representative photomicrographs of ARS stained cells showing the deposition of calcium, and (C) quantification of deposited calcium (normalized to "Ctrl") by hMSCs cultured in monolayer and transfected with released miRNA-20a from hydrogels at days 4, 6, and 8 (D4, D6, and D8, respectively), or freshly reconstituted lyophilized RNA/PEI complexes of siCT ("Neg. Ctrl") or miRNA-20a ("Pos. Ctrl") (RNA 40 nM). "Gel Only": pooled D6 releasates from "UV"-treated hydrogels lacking RNA. # $p < 0.01$ compared to groups that do not contain the same symbol, * $p < 0.05$. The scale bar indicates 200 μm.

differentiation of hMSCs. Quantification of calcium content confirmed increased deposition in the groups transfected with lyophilized or released siNoggin (Figure 8C). Regardless of the absence or presence of UV light exposure, released siNoggin at day 4 (D4) induced calcium deposition to a similar level to "Pos. Ctrl", which exhibited a 3.5-fold increase in calcium mineral deposition compared to the "Ctrl" group. However, a decrease in calcium deposition was observed in groups transfected with siNoggin released at day 6 (D6) and day 8 (D8) from both "UV" and "No UV" hydrogels. This diminution may be due to the presence of higher amounts of hydrogel degradation products containing carboxylic acid groups, which may decrease bioactivity of the released RNA as discussed earlier. A similar reduction in the bioactivity of released siGFP at later time points was observed (Figure 6) and attributed to the presence of hydrogel degradation products in the releasates (Figure S5). Interestingly, there was no significant difference in calcium deposition between cells transfected with released siNoggin from "No UV" and "UV" hydrogels (Figure 8C), indicating that the application of UV to the hydrogels is benign to the loaded siRNA.

In addition to siNoggin, the release of miRNA-20a from 15% (w/w) "Photo-50" hydrogels and the ability of released miRNA-20a to augment osteogenic differentiation of hMSCs in monolayer were also examined. Similar to siNoggin, miRNA-20a released from the photodegradable hydrogels was also accelerated by the application of UV light (Figure 9A). miRNA-20a was released from "UV" and "No UV" hydrogels over the course of 10 and 12 days, respectively. hMSCs in monolayer were treated with the released miRNA-20a, and the cells were then cultured in osteogenic media for 3 weeks before analyzing calcium deposition. miRNA-20a released from the both "No UV" and "UV" hydrogels significantly increased calcium deposition (Figures 9B and 9C) compared to "Ctrl", "Neg. Ctrl" and "Gel Only" groups. Although released miRNA-20a from the "UV" hydrogels exhibited lower amounts of deposited calcium compared to "Pos. Ctrl", there was no significant difference between the groups treated with released miRNA-20a from the "No UV" and "UV" hydrogels at all time points (Figure 9C). These results confirmed that the application of UV light to the hydrogels not only accelerated the release of loaded RNAs but it is also benign to their bioactivity.

4. CONCLUSIONS

We have successfully synthesized photodegradable PEG hydrogels formed via catalyst-free Michael addition reaction for active control of the release of unmodified RNA through UV application. By introducing photodegradable linkages into the hydrogel network, hydrogel swelling ratio and degradation rate were modulated by the application of external UV light and the density of the photodegradable linkage. The release of RNA from the photodegradable PEG hydrogels was sustained and actively accelerated at designated time points by UV stimulation. Released siGFP from these hydrogels exposed to UV or no UV retained its bioactivity as demonstrated by its capacity to silence GFP expression of deGFP-expressing HeLa cells cultured in monolayer. Importantly, this catalyst-free hydrogel permitted encapsulation of cells with high viability,

DOI: 10.1021/acsbiomaterials.6b00796
ACS Biomater. Sci. Eng. 2017, 3, 2011−2023

and the loaded siGFP inhibited the GFP expression of encapsulated deGFP-expressing HeLa cells within the hydrogels. Moreover, released siNoggin and miRNA-20a induced osteogenic differentiation of hMSCs, supporting the potential application of this biomaterial system in tissue engineering strategies. The work provides a platform for spatiotemporal control over the release of other bioactive agents for disease therapeutics and tissue regeneration applications.

■ ASSOCIATED CONTENT

Supporting Information

The Supporting Information is available free of charge on the ACS Publications website at DOI: 10.1021/acsbiomaterials.6b00796.

Synthesis and characterization of PEG-DA and PEG-DPA macromers, effect of siRNA concentration in the prepared siRNA/PEI complexes and subsequent lyophilization on transfection efficiency, effect of hydrogel degradation products on the bioactivity of siRNA, and viability of encapsulated cells in the hydrogels (PDF)

■ AUTHOR INFORMATION

Corresponding Author

*E-mail: eben.alsberg@case.edu. Tel.: +1 216 368 6425. Fax: +1 216 368 4969.

ORCID

Vincent M. Rotello: 0000-0002-5184-5439

Eben Alsberg: 0000-0002-3487-4625

Author Contributions

†C.T.H., Z.Z., and M.K.N. contributed equally to this work.

Notes

The authors declare no competing financial interest.

■ ACKNOWLEDGMENTS

The authors acknowledge funding from the National Institutes of Health (AR069564, AR066193, AR063194 (E.A.), and GM077173 (V.R.)) and the Department of Defense Congressionally Directed Medical Research Programs (OR110196 (E.A.)).

■ REFERENCES

(1) Nguyen, M. K.; Jeon, O.; Krebs, M. D.; Schapira, D.; Alsberg, E. Sustained localized presentation of RNA interfering molecules from in situ forming hydrogels to guide stem cell osteogenic differentiation. *Biomaterials* **2014**, *35* (24), 6278−86.

(2) Andersen, M. O.; Nygaard, J. V.; Burns, J. S.; Raarup, M. K.; Nyengaard, J. R.; Bunger, C.; Besenbacher, F.; Howard, K. A.; Kassem, M.; Kjems, J. siRNA nanoparticle functionalization of nanostructured scaffolds enables controlled multilineage differentiation of stem cells. *Mol. Ther.* **2010**, *18* (11), 2018−27.

(3) Pittenger, M. F.; Mackay, A. M.; Beck, S. C.; Jaiswal, R. K.; Douglas, R.; Mosca, J. D.; Moorman, M. A.; Simonetti, D. W.; Craig, S.; Marshak, D. R. Multilineage potential of adult human mesenchymal stem cells. *Science* **1999**, *284* (5411), 143−147.

(4) Dang, P. N.; Dwivedi, N.; Yu, X.; Phillips, L.; Bowerman, C.; Murphy, W. L.; Alsberg, E. Guiding chondrogenesis and osteogenesis with mineral-coated hydroxyapatite and bmp-2 incorporated within high-density hmsc aggregates for bone regeneration. *ACS Biomater. Sci. Eng.* **2016**, *2* (1), 30−42.

(5) Branch, M. J.; Hashmani, K.; Dhillon, P.; Jones, D. R.; Dua, H. S.; Hopkinson, A. Mesenchymal stem cells in the human corneal limbal stroma. *Invest. Ophthalmol. Visual Sci.* **2012**, *53* (9), 5109−16.

(6) Al-Nbaheen, M.; vishnubalaji, R.; Ali, D.; Bouslimi, A.; Al-Jassir, F.; Megges, M.; Prigione, A.; Adjaye, J.; Kassem, M.; Aldahmash, A. Human stromal (mesenchymal) stem cells from bone marrow, adipose tissue and skin exhibit differences in molecular phenotype and differentiation potential. *Stem Cell Rev. and Rep.* **2013**, *9*, 32−43.

(7) Wang, S.; Qu, X.; Zhao, R. C. Clinical applications of mesenchymal stem cells. *J. Hematol. Oncol.* **2012**, *5*, 19.

(8) Dikina, A. D.; Strobel, H. A.; Lai, B. P.; Rolle, M. W.; Alsberg, E. Engineered cartilaginous tubes for tracheal tissue replacement via self-assembly and fusion of human mesenchymal stem cell constructs. *Biomaterials* **2015**, *52*, 452−62.

(9) Herberg, S.; Aguilar-Perez, A.; Howie, R. N.; Kondrikova, G.; Periyasamy-Thandavan, S.; Elsalanty, M. E.; Shi, X.; Hill, W. D.; Cray, J. J. Mesenchymal stem cell expression of SDF-1β synergizes with BMP-2 to augment cell-mediated healing of critical-sized mouse calvarial defects. *J. Tissue Eng. Regener. Med.* **2015**, DOI: 10.1002/term.2078.

(10) Jeon, O.; Alt, D. S.; Linderman, S. W.; Alsberg, E. Biochemical and physical signal gradients in hydrogels to control stem cell behavior. *Adv. Mater.* **2013**, *25* (44), 6366−72.

(11) Gurkan, U. A.; El Assal, R.; Yildiz, S. E.; Sung, Y.; Trachtenberg, A. J.; Kuo, W. P.; Demirci, U. Engineering anisotropic biomimetic fibrocartilage microenvironment by bioprinting mesenchymal stem cells in nanoliter gel droplets. *Mol. Pharmaceutics* **2014**, *11* (7), 2151−9.

(12) Deng, Y.; Bi, X.; Zhou, H.; You, Z.; Wang, Y.; Gu, P.; Fan, X. Repair of critical-sized bone defects with anti-miR-31-expressing bone marrow stromal stem cells and poly(glycerol sebacate) scaffolds. *Eur. Cell Mater.* **2014**, *27*, 13−24.

(13) Liu, H.; Peng, H.; Wu, Y.; Zhang, C.; Cai, Y.; Xu, G.; Li, Q.; Chen, X.; Ji, J.; Zhang, Y.; OuYang, H. W. The promotion of bone regeneration by nanofibrous hydroxyapatite/chitosan scaffolds by effects on integrin-BMP/Smad signaling pathway in BMSCs. *Biomaterials* **2013**, *34* (18), 4404−17.

(14) Berthiaume, F.; Maguire, T. J.; Yarmush, M. L. Tissue engineering and regenerative medicine: history, progress, and challenges. *Annu. Rev. Chem. Biomol. Eng.* **2011**, *2*, 403−30.

(15) Amado, L. C.; Saliaris, A. P.; Schuleri, K. H.; St. John, M.; Xie, J. S.; Cattaneo, S.; Durand, D. J.; Fitton, T.; Kuang, J. Q.; Stewart, G.; Lehrke, S.; Baumgartner, W. W.; Martin, B. J.; Heldman, A. W.; Hare, J. M. Cardiac repair with intramyocardial injection of allogeneic mesenchymal stem cells after myocardial infarction. *Proc. Natl. Acad. Sci. U. S. A.* **2005**, *102* (32), 11474−9.

(16) Mehta, M.; Schmidt-Bleek, K.; Duda, G. N.; Mooney, D. J. Biomaterial delivery of morphogens to mimic the natural healing cascade in bone. *Adv. Drug Delivery Rev.* **2012**, *64* (12), 1257−76.

(17) Elsabahy, M.; Nazarali, A.; Foldvari, M. Non-viral nucleic acid delivery: key challenges and future directions. *Curr. Drug Delivery* **2011**, *8* (3), 235−44.

(18) Nguyen, M. K.; Alsberg, E. Bioactive factor delivery strategies from engineered polymer hydrogels for therapeutic medicine. *Prog. Polym. Sci.* **2014**, *39* (7), 1235−65.

(19) Gavrilov, K.; Saltzman, W. M. Therapeutic siRNA: principles, challenges, and strategies. *Yale J. Biol. Med.* **2012**, *85* (2), 187−200.

(20) Aagaard, L.; Rossi, J. J. RNAi therapeutics: principles, prospects and challenges. *Adv. Drug Delivery Rev.* **2007**, *59* (2−3), 75−86.

(21) Kim, W. J.; Kim, S. W. Efficient siRNA delivery with non-viral polymeric vehicles. *Pharm. Res.* **2009**, *26* (3), 657−66.

(22) Beavers, K. R.; Nelson, C. E.; Duvall, C. L. MiRNA inhibition in tissue engineering and regenerative medicine. *Adv. Drug Delivery Rev.* **2015**, *88*, 123−37.

(23) Tabernero, J.; Shapiro, G. I.; LoRusso, P. M.; Cervantes, A.; Schwartz, G. K.; Weiss, G. J.; Paz-Ares, L.; Cho, D. C.; Infante, J. R.; Alsina, M.; Gounder, M. M.; Falzone, R.; Harrop, J.; White, A. C.; Toudjarska, I.; Bumcrot, D.; Meyers, R. E.; Hinkle, G.; Svrzikapa, N.; Hutabarat, R. M.; Clausen, V. A.; Cehelsky, J.; Nochur, S. V.; Gamba-Vitalo, C.; Vaishnaw, A. K.; Sah, D. W.; Gollob, J. A.; Burris, H. A., III First-in-humans trial of an RNA interference therapeutic targeting

VEGF and KSP in cancer patients with liver involvement. *Cancer Discovery* **2013**, *3* (4), 406−17.
(24) Navarro, G.; Sawant, R. R.; Biswas, S.; Essex, S.; Tros de Ilarduya, C.; Torchilin, V. P. P-glycoprotein silencing with siRNA delivered by DOPE-modified PEI overcomes doxorubicin resistance in breast cancer cells. *Nanomedicine* **2012**, *7* (1), 65−78.
(25) Han, L.; Tang, C.; Yin, C. Enhanced antitumor efficacies of multifunctional nanocomplexes through knocking down the barriers for siRNA delivery. *Biomaterials* **2015**, *44*, 111−21.
(26) Segovia, N.; Pont, M.; Oliva, N.; Ramos, V.; Borros, S.; Artzi, N. Hydrogel doped with nanoparticles for local sustained release of siRNA in breast cancer. *Adv. Healthcare Mater.* **2015**, *4*, 271−80.
(27) Park, H.; Ku, S. H.; Park, H.; Hong, J.; Kim, D.; Choi, B.-R.; Pak, H.-N.; Lee, M.-H.; Mok, H.; Jeong, J. H.; Choi, D.; Kim, S. H.; Joung, B. RAGE siRNA-mediated gene silencing provides cardioprotection against ventricular arrhythmias in acute ischemia and reperfusion. *J. Controlled Release* **2015**, *217*, 315−26.
(28) Zhang, J. F.; Fu, W. M.; He, M. L.; Xie, W. D.; Lv, Q.; Wan, G.; Li, G.; Wang, H.; Lu, G.; Hu, X.; Jiang, S.; Li, J. N.; Lin, M. C.; Zhang, Y. O.; Kung, H. F. miRNA-20a promotes osteogenic differentiation of human mesenchymal stem cells by co-regulating BMP signaling. *RNA Biol.* **2011**, *8* (5), 829−38.
(29) Nelson, C. E.; Kim, A. J.; Adolph, E. J.; Gupta, M. K.; Yu, F.; Hocking, K. M.; Davidson, J. M.; Guelcher, S. A.; Duvall, C. L. Tunable delivery of siRNA from a biodegradable scaffold to promote angiogenesis in vivo. *Adv. Mater.* **2014**, *26* (4), 607−14.
(30) Heliotis, M.; Tsiridis, E. Suppression of bone morphogenetic protein inhibitors promotes osteogenic differentiation: therapeutic implications. *Arthritis Res. Ther.* **2008**, *10* (4), 115.
(31) Bassit, A. C. F.; Moffatt, P.; Gaumond, M.-H.; Hamdy, R. The potential use of nanoparticles for noggin sirna delivery to accelerate bone formation in distraction osteogenesis. *J. Nanomed. Nanotechnol.* **2015**, *6* (1), 257.
(32) Nelson, C. E.; Gupta, M. K.; Adolph, E. J.; Guelcher, S. A.; Duvall, C. L. siRNA delivery from an injectable scaffold for wound therapy. *Adv. Wound Care.* **2013**, *2* (3), 93−9.
(33) Charafeddine, R. A.; Makdisi, J.; Schairer, D.; O'Rourke, B. P.; Diaz-Valencia, J. D.; Chouake, J.; Kutner, A.; Krausz, A.; Adler, B.; Nacharaju, P.; Liang, H.; Mukherjee, S.; Friedman, J. M.; Friedman, A.; Nosanchuk, J. D.; Sharp, D. J. Fidgetin-Like 2: A microtubule-based regulator of wound healing. *J. Invest. Dermatol.* **2015**, *135* (9), 2309−18.
(34) Lin, T.-H.; Yang, R.-S.; Tang, C.-H.; Lin, C.-P.; Fu, W.-M. PPARγ inhibits osteogenesis via the down-regulation of the expression of COX-2 and iNOS in rats. *Bone* **2007**, *41* (4), 562−74.
(35) Lee, H.; Lytton-Jean, A. K.; Chen, Y.; Love, K. T.; Park, A. I.; Karagiannis, E. D.; Sehgal, A.; Querbes, W.; Zurenko, C. S.; Jayaraman, M.; Peng, C. G.; Charisse, K.; Borodovsky, A.; Manoharan, M.; Donahoe, J. S.; Truelove, J.; Nahrendorf, M.; Langer, R.; Anderson, D. G. Molecularly self-assembled nucleic acid nanoparticles for targeted in vivo siRNA delivery. *Nat. Nanotechnol.* **2012**, *7* (6), 389−93.
(36) Zhang, Y.; Wang, Z.; Gemeinhart, R. A. Progress in microRNA delivery. *J. Controlled Release* **2013**, *172* (3), 962−74.
(37) Rettig, G. R.; Behlke, M. A. Progress toward in vivo use of siRNAs-II. *Mol. Ther.* **2012**, *20* (3), 483−512.
(38) Behlke, M. A. Progress towards in vivo use of siRNAs. *Mol. Ther.* **2006**, *13* (4), 644−70.
(39) Hobel, S.; Aigner, A. Polyethylenimines for siRNA and miRNA delivery in vivo. *WIREs Nanomed. Nanobiotechnol.* **2013**, *5* (5), 484−501.
(40) Whitehead, K. A.; Dahlman, J. E.; Langer, R. S.; Anderson, D. G. Silencing or stimulation? siRNA delivery and the immune system. *Annu. Rev. Chem. Biomol. Eng.* **2011**, *2*, 77−96.
(41) Chen, M.; Gao, S.; Dong, M.; Song, J.; Yang, C.; Howard, K. A.; Kjems, J.; Besenbacher, F. Chitosan/siRNA nanoparticles encapsulated in PLGA nanofibers for siRNA delivery. *ACS Nano* **2012**, *6* (6), 4835−44.
(42) Foster, A. A.; Greco, C. T.; Green, M. D.; Epps, T. H., III; Sullivan, M. O. Light-mediated activation of sirna release in diblock copolymer assemblies for controlled gene silencing. *Adv. Healthcare Mater.* **2015**, *4* (5), 760−70.
(43) Nguyen, K.; Dang, P. N.; Alsberg, E. Functionalized, biodegradable hydrogels for control over sustained and localized siRNA delivery to incorporated and surrounding cells. *Acta Biomater.* **2013**, *9* (1), 4487−95.
(44) Krebs, M. D.; Jeon, O.; Alsberg, E. Localized and sustained delivery of silencing RNA from macroscopic biopolymer hydrogels. *J. Am. Chem. Soc.* **2009**, *131* (26), 9204−6.
(45) Krebs, M. D.; Alsberg, E. Localized, targeted, and sustained siRNA delivery. *Chem. - Eur. J.* **2011**, *17* (11), 3054−62.
(46) Huynh, C. T.; Nguyen, Q. V.; Lym, J. S.; Kim, B. S.; Huynh, D. P.; Jae, H. J.; Kim, Y. I.; Lee, D. S. Intraarterial gelation of injectable cationic pH/temperature-sensitive radiopaque embolic hydrogels in a rabbit hepatic tumor model and their potential application for liver cancer treatment. *RSC Adv.* **2016**, *6* (53), 47687−97.
(47) Huynh, C. T.; Nguyen, M. K.; Lee, D. S. Dually cationic and anionic pH/temperature-sensitive injectable hydrogels and potential application as a protein carrier. *Chem. Commun.* **2012**, *48* (89), 10951−3.
(48) Samorezov, J. E.; Alsberg, E. Spatial regulation of controlled bioactive factor delivery for bone tissue engineering. *Adv. Drug Delivery Rev.* **2015**, *84*, 45−67.
(49) Loh, X. J.; Guerin, W.; Guillaume, S. M. Sustained delivery of doxorubicin from thermogelling poly (PEG/PPG/PTMC urethane) s for effective eradication of cancer cells. *J. Mater. Chem.* **2012**, *22* (39), 21249−56.
(50) Han, H. D.; Mora, E. M.; Roh, J. W.; Nishimura, M.; Lee, S. J.; Stone, R. L.; Bar-Eli, M.; Lopez-Berestein, G.; Sood, A. K. Chitosan hydrogel for localized gene silencing. *Cancer Biol. Ther.* **2011**, *11* (9), 839−45.
(51) Lym, J. S.; Nguyen, Q. V.; Ahn, D. W.; Huynh, C. T.; Jae, H. J.; Kim, Y. I.; Lee, D. S. Sulfamethazine-based pH-sensitive hydrogels with potential application for transcatheter arterial chemoembolization therapy. *Acta Biomater.* **2016**, *41*, 253−63.
(52) Nguyen, Q. V.; Lym, J. S.; Huynh, C. T.; Kim, B. S.; Jae, H. J.; Kim, Y. I.; Lee, D. S. Novel sulfamethazine-based pH-sensitive copolymer for injectable radiopaque embolic hydrogel and potential application in hepatocellular carcinoma therapy. *Polym. Chem.* **2016**, *7*, 5805−5818.
(53) Jeon, O.; Wolfson, D. W.; Alsberg, E. In-situ formation of growth-factor-loaded coacervate microparticle-embedded hydrogels for directing encapsulated stem cell fate. *Adv. Mater.* **2015**, *27* (13), 2216−23.
(54) Ren, K.; He, C.; Xiao, C.; Li, G.; Chen, X. Injectable glycopolypeptide hydrogels as biomimetic scaffolds for cartilage tissue engineering. *Biomaterials* **2015**, *51*, 238−49.
(55) Drury, J. L.; Mooney, D. J. Hydrogels for tissue engineering: scaffold design variables and applications. *Biomaterials* **2003**, *24* (24), 4337−51.
(56) Hoffman, A. S. Hydrogels for biomedical applications. *Adv. Drug Delivery Rev.* **2012**, *64*, 18−23.
(57) Yin, L.; Zhao, X.; Ji, S.; He, C.; Wang, G.; Tang, C.; Gu, S.; Yin, C. The use of gene activated matrix to mediate effective SMAD2 gene silencing against hypertrophic scar. *Biomaterials* **2014**, *35* (8), 2488−98.
(58) Hill, M. C.; Nguyen, M. K.; Jeon, O.; Alsberg, E. Spatial control of cell gene expression by sirna gradients in biodegradable hydrogels. *Adv. Healthcare Mater.* **2015**, *4* (5), 714−22.
(59) Nelson, C. E.; Gupta, M. K.; Adolph, E. J.; Shannon, J. M.; Guelcher, S. A.; Duvall, C. L. Sustained local delivery of siRNA from an injectable scaffold. *Biomaterials* **2012**, *33* (4), 1154−61.
(60) Kim, Y. M.; Park, M. R.; Song, S. C. An injectable cell penetrable nano-polyplex hydrogel for localized siRNA delivery. *Biomaterials* **2013**, *34* (18), 4493−500.
(61) Nguyen, M. K.; McMillan, A.; Huynh, C. T.; Schapira, D. S.; Alsberg, E. Photocrosslinkable, biodegradable hydrogels with controlled cell adhesivity for prolonged siRNA delivery to hMSCs to

DOI: 10.1021/acsbiomaterials.6b00796
ACS Biomater. Sci. Eng. 2017, 3, 2011−2023

enhance their osteogenic differentiation. *J. Mater. Chem. B* **2017**, *5* (3), 485−495.
(62) Huynh, C. T.; Nguyen, M. K.; Tonga, G. Y.; Longe, L.; Rotello, V. M.; Alsberg, E. Photocleavable hydrogels for light-triggered siRNA release. *Adv. Healthcare Mater.* **2016**, *5* (3), 305−10.
(63) Huynh, C. T.; Nguyen, M. K.; Naris, M.; Tonga, G. Y.; Rotello, V. M.; Alsberg, E. Light-triggered RNA release and induction of hMSC osteogenesis via photodegradable, dual-crosslinked hydrogels. *Nanomedicine* **2016**, *11* (12), 1535−50.
(64) Kharkar, P. M.; Kiick, K. L.; Kloxin, A. M. Design of Thiol- and Light-sensitive Degradable Hydrogels using Michael-type Addition Reactions. *Polym. Chem.* **2015**, *6* (31), 5565−74.
(65) Tibbitt, M. W.; Han, B. W.; Kloxin, A. M.; Anseth, K. S. Synthesis and application of photodegradable microspheres for spatiotemporal control of protein delivery. *J. Biomed. Mater. Res., Part A* **2012**, *100* (7), 1647−54.
(66) Huynh, C. T.; Lee, D. S. Controlling the properties of poly(amino ester urethane)-poly(ethylene glycol)-poly(amino ester urethane) triblock copolymer pH/temperature-sensitive hydrogel. *Colloid Polym. Sci.* **2012**, *290* (11), 1077−86.
(67) Jin, R.; Moreira Teixeira, L. S.; Dijkstra, P. J.; Karperien, M.; van Blitterswijk, C. A.; Zhong, Z. Y.; Feijen, J. Injectable chitosan-based hydrogels for cartilage tissue engineering. *Biomaterials* **2009**, *30* (13), 2544−51.
(68) Huynh, N.-T.; Jeon, Y.-S.; Kim, D.; Kim, J.-H. Preparation and swelling properties of "click" hydrogel from polyaspartamide derivatives using tri-arm PEG and PEG-co-poly(amino urethane) azides as crosslinking agents. *Polymer* **2013**, *54* (4), 1341−9.
(69) Kloxin, A. M.; Kasko, A. M.; Salinas, C. N.; Anseth, K. S. Photodegradable hydrogels for dynamic tuning of physical and chemical properties. *Science* **2009**, *324* (5923), 59−63.
(70) Larsen, S. A.; Kassem, M.; Rattan, S. I. Glucose metabolite glyoxal induces senescence in telomerase-immortalized human mesenchymal stem cells. *Chem. Cent. J.* **2012**, *6* (1), 18.
(71) Gregory, C. A.; Gunn, W. G.; Peister, A.; Prockop, D. J. An Alizarin red-based assay of mineralization by adherent cells in culture: comparison with cetylpyridinium chloride extraction. *Anal. Biochem.* **2004**, *329* (1), 77−84.
(72) Stanford, C. M.; Jacobson, P. A.; Eanes, E. D.; Lembke, L. A.; Midura, R. J. Rapidly forming apatitic mineral in an osteoblastic cell line (UMR 10601 BSP). *J. Biol. Chem.* **1995**, *270* (16), 9420−9428.
(73) Jeon, O.; Powell, C.; Ahmed, S. M.; Alsberg, E. Biodegradable, photocrosslinked alginate hydrogels with independently tailorable physical properties and cell adhesivity. *Tissue Eng., Part A* **2010**, *16* (9), 2915−25.
(74) Nguyen, Q. V.; Huynh, D. P.; Park, J. H.; Lee, D. S. Injectable polymeric hydrogels for the delivery of therapeutic agents: A review. *Eur. Polym. J.* **2015**, *72*, 602−19.
(75) Dey, P.; Hemmati-Sadeghi, S.; Haag, R. Hydrolytically degradable, dendritic polyglycerol sulfate based injectable hydrogels using strain promoted azide-alkyne cycloaddition reaction. *Polym. Chem.* **2016**, *7* (2), 375−83.
(76) Bosio, V.; Dubreuil, F.; Bogdanovic, G.; Fery, A. Interactions between silica surfaces coated by polyelectrolyte multilayers in aqueous environment: comparison between precursor and multilayer regime. *Colloids Surf., A* **2004**, *243* (1−3), 147−55.
(77) Meneksedag-Erol, D.; Tang, T.; Uludag, H. Probing the effect of miRNA on siRNA-PEI polyplexes. *J. Phys. Chem. B* **2015**, *119* (17), 5475−86.
(78) Gratton, S. E. A.; Ropp, P. A.; Pohlhaus, P. D.; Luft, J. C.; Madden, V. J.; Napier, M. E.; DeSimone, J. M. The effect of particle design on cellular internalization pathways. *Proc. Natl. Acad. Sci. U. S. A.* **2008**, *105* (33), 11613−8.

DOI: 10.1021/acsbiomaterials.6b00796
ACS Biomater. Sci. Eng. 2017, 3, 2011−2023